

## ***In situ* compatibilization of polylactide/thermoplastic polyester elastomer blends using a multifunctional epoxide compound as a processing agent**

Sisi Wang,<sup>1,2</sup> Sujuan Pang,<sup>1,2</sup> Nai Xu,<sup>1,2</sup> Lisha Pan,<sup>1,2</sup> Qiang Lin<sup>3</sup>

<sup>1</sup>College of Materials and Chemical Engineering, Hainan University, Haikou, Hainan 570228, China

<sup>2</sup>Hainan Provincial Fine Chemical Engineering Research Center, Hainan University, Haikou, Hainan 570228, China

<sup>3</sup>College of Chemistry and Chemical Engineering, Hainan Normal University, Haikou, Hainan 571158, China

Correspondence to: Nai Xu (E-mail: xunai@hainu.edu.cn)

**ABSTRACT:** *In situ* compatibilized poly(lactic acid)/thermoplastic polyester elastomer (PLA/TPEE) (80/20) blends are prepared by using multifunctional epoxide oligomer (coded as ADR) as a reactive modifier. Experiments such as torque, melt mass flow rate (MFR), SEM, DSC and tensile test were conducted to characterize properties of the PLA/TPEE/ADR blends. *In situ* reactions between PLA, TPEE and ADR were researched using a lab torque rheometer. It was proposed that ADR may initiate a variety of chain extension/branching reactions between PLA and TPEE under mixing process. In particular, the formed copolymer PLA-ADR-TPEE could be viewed as an *in situ* compatibilizer to improve the compatibility of PLA and TPEE. As expected, the value of MFR decreased greatly with increasing the ADR addition. The morphology reveals that interface adhesion of PLA/TPEE blend was enhanced with the incorporation of ADR, which led to a reduction in TPEE domain size. Moreover, tensile ductility of PLA/TPEE (80/20) blend was improved greatly by addition of the reactive modifier, e.g. the elongation at break was increased from 53% to the maximum value of 213% with addition of 1.2 phr ADR. The toughening effect can be explained by crazing with shear yielding mechanism. Attempts were made to produce ductile films from these PLA/TPEE/ADR blends by using extrusion blowing method. Effect of ADR on blowing stability and tensile property of these blends was investigated. Improvement on blowing stability and tensile ductility of PLA/TPEE/ADR films also shows that ADR is an efficiently reactive compatibilizer, as well as a viscosity enhancer for PLA/TPEE blends. © 2016 Wiley Periodicals, Inc. *J. Appl. Polym. Sci.* **2016**, *133*, 43424.

**KEYWORDS:** biopolymers & renewable polymers; compatibilization; elastomers; mechanical properties; morphology

Received 3 September 2015; accepted 7 January 2016

DOI: 10.1002/app.43424

### **INTRODUCTION**

Bio-based and biodegradable poly(lactic acid) (PLA) has been received considerable attention in the past decades due to the sustainable and environmental issues resulted from conventional petroleum-based polymers.

PLA is an attractive candidate for replacing petrochemical polymers due to its biocompatibility, biodegradability and renewability.<sup>1–3</sup> PLA has reasonably good mechanical, optical and barrier properties compared to general petroleum-based polymers. The growing demands for PLA can be expected for many applications, such as household field, industry, biomedical items, etc. In particular, PLA is universally acknowledged as an ideal substitute for petroleum-based polymers to fabricate environmental packaging films.

However, inherent brittleness of PLA greatly limits its applications.<sup>1,2</sup> Blending with some elastomers or flexible resins such as polyur-

ethane,<sup>4</sup> poly(ethylene oxide-*b*-amide-12),<sup>5</sup> poly(3-hydroxybutyrate-co-4-hydroxybutyrate),<sup>6</sup> poly(caprolactone),<sup>7</sup> poly(butylene succinate),<sup>8</sup> and poly(butylene adipate-co-terephthalate),<sup>9</sup> is an effective and economical method to improve the ductility of PLA. Of course, most of these PLA blends belong to incompatible blending systems. And the poor compatibility between components would largely undermine the toughness effect of elastomers on PLA matrix. Hence, some compatibilizers often are used to enhance the compatibility of PLA blends.<sup>2</sup>

Thermoplastic elastomers (TPEs) are growing in importance as a novel polymer material which covers the boundary between rubber and plastic. Notably, thermoplastic polyester elastomer (TPEE) among TPEs has good comprehensive property of strength, flexibility and processing performance.<sup>10</sup> TPEE is a block copolymer with soft segments of poly(tetramethylene ether) glycol terephthalate blocks and hard segments of polybutylene terephthalate blocks.<sup>11</sup>

Increase of the hard segment ratio can enhance the physical rigidity and chemical stability. Conversely, increasing soft segment proportion can improve the flexibility and dynamic mechanical properties. In view of its good performance, TPEE is considered as a good candidate for the toughening of PLA.

So far, few studies of PLA/TPEE blend have been reported in literature. Haydar U. Zaman *et al.*<sup>10</sup> researched the toughening effect of TPEE on PLA. The authors found that the compatibility between PLA and TPEE was poor which greatly limited the improvement on ductility of PLA/TPEE blends. In order to enhance the compatibility of PLA/TPEE blends, a diisocyanate compound (methylene diphenyl diisocyanate, MDI) was used as a reactive modifier because diisocyanates are highly reactive with both hydroxyl and carboxyl end groups of PLA and TPEE. It was found that melt blending of PLA and TPEE with MDI did not lead to an obvious drop in tensile strength and modulus whereas the elongation at break showed a significant increase (340%) when compared with neat PLA and PLA/TPEE blend. The relative tensile ductility of PLA/TPEE/MDI is 34 times higher than that of neat PLA. The brittle fracture of neat PLA was transformed into a ductile fracture by the addition of MDI.

However, the toxicity and volatility of diisocyanate compounds would largely limit the application of these modified PLA/TPEE blends in household, food and medical packaging fields.

Recently, multifunctional chain extenders containing epoxy groups have been used in PLA and its blends.<sup>2,12–15</sup> These chain extenders have been developed to improve melt strength, thermal stability as well as to work as compatibilizers in PLA blends. Theoretically, the epoxy groups in the chain extender may react with the carboxyl and hydroxyl terminal groups of polyester blends, that will cause an increase in the molecular weight and a formation of copolymers in polyester blends during compounding in the molten state. The copolymer *in situ* generated can work as a physical compatibilizer to improve the compatibility and physical properties of polyester blends. Zhang *et al.*<sup>12</sup> incorporated a copolymer of ethylene, acrylic and glycidyl methacrylate (T-GMA) into PLA/PBAT blends as a reactive processing agent. It was found that the PLA/PBAT/T-GMA blends showed better miscibility and higher hardness without severe loss in tensile strength. Racha Al-Itiry *et al.*<sup>13</sup> reported an improvement of mechanical performance and thermal stability of PLA/PBAT blends using multifunctional epoxide Joncryl ADR-4368 as a chain extender, as well as a reactive compatibilizer. The improved mechanical properties indicate a reactivity control at the interface due to the formation of ester linkages between PLA, PBAT and ADR-4368. The effect of reactive compatibilization on the PLA/PBAT blends was confirmed using TEM, SEM observations and tensile tests by the improvement of phase dispersion and the increase of tensile ductility. The similar compatibilization effect of ADR-4368 on PLA/PBAT blends was also reported by Arruda *et al.*<sup>14</sup> Zhang *et al.* researched the compatibility effect of multifunctional epoxide on immiscible PLA/EVOH blends.<sup>15</sup> It was found that the multifunctional epoxide showed a poor reactive compatibility effect due to low reaction activity between the epoxy groups in multifunctional epoxide and the hydroxyl groups in EVOH. The authors successfully enhanced the reactive activity of epoxy

groups and hydroxyl groups by using zinc stearate (ZnSt<sub>2</sub>) as a catalyst. The compatibilization effect caused by the multifunctional epoxide and ZnSt<sub>2</sub> significantly reduced the EVOH domain size, and the interfaces became very fuzzy. The dynamic light scattering measurement showed that the diameter of EVOH particles ranged from 100 to 500 nm, much smaller than that of those blends without the catalyst. As a result, the transparency and barrier property to water vapor of these compatibilized blends were significantly improved.

In this article, a low toxic and nonvolatile multifunctional epoxide oligomer (supplied by BASF, coded as Joncryl ADR<sup>®</sup>-4370s) was used as a reactive modifier to enhance the compatibility and ductility of PLA/TPEE blends. (Joncryl ADR<sup>®</sup>-4370s was referred as ADR in this study unless specified.)

A lab torque rheometer was used to investigate the reactions between PLA, TPEE and ADR during compounding in the molten state. The effect of ADR addition on melt flow property of PLA/TPEE/ADR blends was measured using a melt mass rate flow meter. The morphology, tensile property and thermal behavior of PLA/TPEE/ADR blends were researched. And the reactive compatibility and toughening mechanism of PLA/TPEE/ADR blends were proposed. In addition, film blowing processes for PLA/TPEE (80/20) and PLA/TPEE/ADR (80/20/x) blends were researched preliminarily. The effect of chain extension/branching reaction and compatibilization phenomenon generated by ADR on the stability flow during blowing extrusion process and the tensile property of films for these PLA blends was studied.

## EXPERIMENTAL

### Materials

PLA pellets supplied by NatureWorks LLC is a semicrystalline grade (4032D) comprising around 2% D-lactide units. The value of melt mass flow rate of PLA pellets (190 °C under 2.16 kg load) is 3.3 g·10 min<sup>-1</sup>, and its density is 1.25 g/cm<sup>3</sup>.

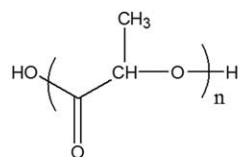
TPEE pellets (4056) were obtained commercially from DuPont with the given properties: density = 1.11 g/cm<sup>3</sup>, hardness = 37 Shore D, stress at break = 26 MPa, elongation at break = 886%, and melt mass flow rate = 6.0 g·10 min<sup>-1</sup> (190 °C under 2.16 kg load).

Commercial available multifunctional epoxide, Joncryl ADR<sup>®</sup>-4370s was purchased from BASF with an epoxy equivalent weight of 285 g/mol and a molecular weight of 6800 g/mol. It is a kind of transparent solid powder, generally used as chain extender, copolymerized by styrene and acrylate monomers. In this article, Joncryl ADR<sup>®</sup>-4370s is abbreviated as ADR.

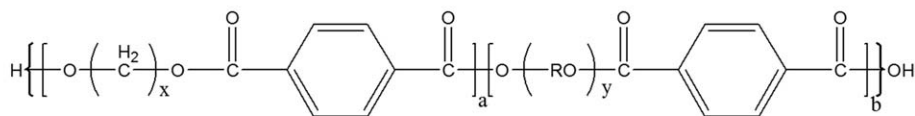
The chemical structures of PLA, TPEE and ADR are shown in Figure 1.

### Sample Preparation

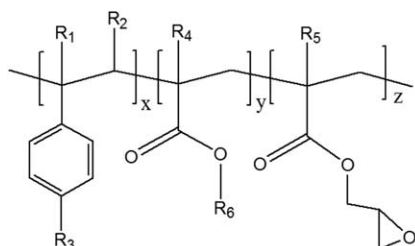
PLA and TPEE pellets were dried in a vacuum oven at 50 °C for 12 h prior to processing. The PLA/TPEE/ADR blends were prepared by melt mixing using a lab torque rheometer (XSS300, Shanghai Kechuang Plastic Machinery Factory, China). Firstly, a certain amount of ADR powders, PLA and TPEE pellets were added into the mixing chamber quickly at 190 °C with a rotor speed of 50 rpm. After the blends in mixing chamber melted completely, the PLA/TPEE/ADR melts had been subsequently



(A) PLA



(B) TPEE



ADR: General structure of the styrene-acrylic multi-functional oligomeric chain extenders. Where R1-R5 are H, CH<sub>3</sub>, a higher alkyl group, or combinations of them; R<sub>6</sub> is an alkyl group, and x, y and z are each between 1 and 20.

(C) ADR

Figure 1. The chemical structures of PLA, TPEE, and ADR.

blended at 190 °C for 10 min with a rotor speed of 50 rpm. Then, the melts were air cooled quickly, and the obtained blends were kept for tensile specimens preparation and MFR test. These PLA blends were molded into sheets with a thickness of 1 mm. And then, the sheets were cut into some standard dumbbell shaped specimens for following tensile test. Molding was carried out at 210 °C under 15 MPa for 8 min. Exhausting twice during the hot pressing. Then the specimens were quenched between two cold plates with a water cooling system under 15 MPa.

Here, the resulted blends are referred as PLA/TPEE/ADR (80/20/x), where the weight ratio of PLA/TPEE is kept to be 80/20. And x denotes ADR parts per hundreds of total resin (phr). In this article, x is 0, 0.3, 0.6, 0.9, and 1.2 phr, respectively.

To investigate the chain extension effect of ADR on MFR and molecular weight of neat PLA and neat TPEE, PLA/ADR (100/x) and TPEE/ADR (100/x) with various ADR loadings were also prepared under the same processing condition.

To make sure neat PLA and TPEE resins undergo the same processing and thermal history, neat PLA and TPEE melts were also processed at 190 °C for 10 min with a rotor speed of 50 rpm, respectively.

#### Blowing Extrusion Process

The blown films were prepared in a single screw extruder (LSJ-20, Shanghai Kechuang Plastic Machinery Factory, China) with 20 mm diameter screw, L/D 25. An annular die of 34.0 mm

diameter, with die gap of 0.5 mm was used to shape the initial tube dimensions. The processing temperature at different zones was set from 170 to 185 °C. The screw speed in the film extruder was of 20 rpm. The take-up speed was set to 1.65 m/min. When the blowing extrusion process started up, pressure-air was introduced at the bottom of the die to inflate the initial tube and form a bubble. The size of the bubble was maintained at a certain internal pressure. And then, the tube was flattened in the nip rolls and taken up by the winder. Finally, a roll of film was obtained. A more detailed description of the blowing extrusion process was presented in the literature.<sup>3</sup> In this experiment, the obtained films have a mean thickness ranged from 40 to 50 μm and a blow-up ratio (ratio of bubble diameter to die diameter) of around 2:1.

#### Torque

A certain amount of PLA, TPEE, PLA/TPEE, respectively, were blended with quantitative ADR in an internal mixer of XSS-300 torque rheometer, which was controlled steadily at a temperature of 190 °C ± 2 °C and rotated at 50 rpm. The total mixing time was set at 30 min. And the melt torque during mixing was recorded as a function of time in order to measure extent of the chain extension reaction and thermal stability of the melt.

Firstly, in order to confirm the chain extension reaction of ADR with PLA and TPEE, melt torques vs. time plots for PLA/ADR (100/x) and TPEE/ADR (100/x) with various ADR loading were recorded. And then, the melt torques vs. time plots for

PLA/TPEE/ADR (80/20/*x*) blends were also recorded. Here, *x* is 0, 0.3, 0.6, 0.9, and 1.2 phr, respectively.

#### Melt Mass Flow Rate (MFR)

MFR measurement was performed to investigate the effect of ADR loading on the melt viscosity of PLA/TPEE (80/20) blend, as well as neat PLA and TPEE. It was tested on a melt index tester (XNR-400B, Chengde City Desheng instrument co., LTD). The MFR test was carried out at 190 °C under 2.16 kg load.

#### Size Exclusion Chromatography (SEC)

Average molecular weights and polydispersity index (PDI) of PLA, as well as for TPEE, before and after processing were measured using a Waters 515 gel permeation chromatography system. Furthermore, to investigate the chain extension effect of ADR, the average molecular weights and PDI of PLA/ADR and TPEE/ADR samples were measured also. Tetrahydrofuran (HPLC grade) was used as a solvent and an eluent at a flow rate of 2 ml/min. Number-average molecular weight ( $M_n$ ) and weight-average molecular weight ( $M_w$ ) were determined from calibration plots constructed with polystyrene standards.

#### Morphology

Scanning electron microscopy (SEM) (S-3500N, Hitachi, Japan) was conducted in order to observe morphology of cryo-fracture surfaces and distribution of TPEE domains in PLA matrix. Sample surfaces were previously fractured after immersion in liquid nitrogen for enough time and then coated with a thin layer of gold to avoid electrostatic charging and provide conductive surfaces. An acceleration voltage of 10 kV was used for all observations.

#### Tensile Property

Tensile tests were performed on a XLW intelligent electronic tensile testing machine (Jinan Languang mechanical and electrical technology co., LTD), equipped with a 500 N load cell. The tensile strength ( $\sigma$ ) and elongation at break ( $\epsilon$ ) of these dumb-bell shaped specimens for PLA blends were measured. Eight replicates were tested for each sample to get an average value. A crosshead speed of 50 mm/min was used.

In addition, tensile properties of the blown films also were tested. And a crosshead speed of 50 mm/min was used. Rectangular specimens with a width of 15 mm were cut from the blown film with the length parallel to the take-up direction or machine direction (MD), and with the length transversal to the take-up direction (TD), respectively.

#### Thermal Analysis

The crystallization and melting behaviors of samples were investigated using a differential scanning calorimeter (Q100, TA instrument) equipped with a liquid nitrogen cooling system. The DSC cell was constantly purged with nitrogen at a flow rate of 50 mL/min. The measurements were made using  $5.00 \pm 0.50$  mg samples. A set of heating/cooling ramps was carried out following a three step process. Samples were first heated to 200 °C at a rate of 50 °C/min and held at 200 °C for 4 min to erase the thermal history of the material, then cooled down to 20 °C at 10 °C/min. Finally, they were heated back to 200 °C with a scan rate of 10 °C/min to record the cold crystallization and melting behavior. Glass transition temperature ( $T_g$ ), cold crystallization temperature ( $T_c$ ), and melting temperature ( $T_m$ ) were determined in the second heating scan.

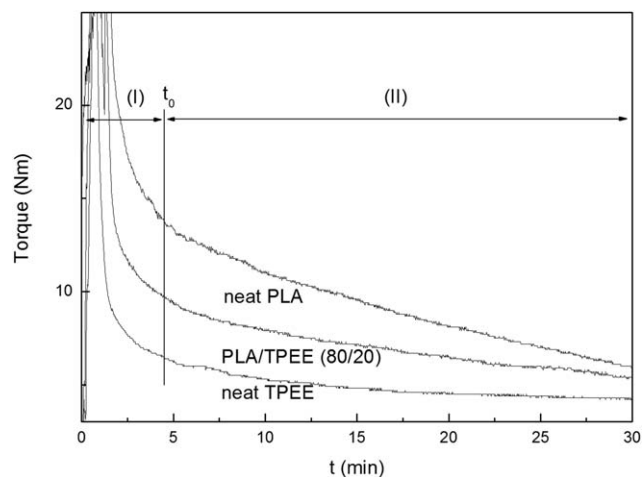


**Figure 2.** Melt torque as a function of time for neat PLA, neat TPEE, and PLA/TPEE (80/20) blend.

The percent crystallinity ( $X_c$ ) was calculated by using eq. (1):

$$X_c = 100 \times \frac{|\Delta H_m| - |\Delta H_{cc}|}{W_{PLA} \cdot |\Delta H_m^0|} \quad (1)$$

where  $W_{PLA}$  is the weight fraction of PLA matrix, while  $\Delta H_m^0$  is melting enthalpy of 100% crystalline PLA given as 93 J/g in the literature.<sup>16</sup>  $\Delta H_m$  and  $\Delta H_{cc}$  are melting enthalpy and cold crystallization enthalpy of PLA matrix in PLA/TPEE/ADR (80/20/*x*) samples, respectively.

## RESULTS AND DISCUSSION

### Chain Extension and Coupling Reaction with ADR in a Torque Rheometer

Theoretically, being a multifunctional epoxide compound, ADR not only can be used as a chain extender, but also as a reactive compatibilizer in PLA/TPEE blending system. Hence, a lab torque rheometer was used to confirm the coupling effects of ADR on neat PLA, TPEE and PLA/TPEE (80/20) blend, respectively. The torque versus mixing time was monitored over a prolonged time (30 min) in order to follow the evolution of these reactions at 190 °C. To compare the chain extension and coupling results, first, blank runs were performed with neat PLA, TPEE and PLA/TPEE (80/20), respectively. And these initial melt torques were recorded, as shown in Figure 2. These torque vs. time plots for blank resins can be divided into two sections. The first (I) regime between 0 and 4.5 min corresponds to feeding and melting process of resins in the mixing chamber. After the initial melting period, the torques of these blank melts show a continuous decrease in the second (II) regime. As expected, the continuous decrease in the torque values is attributed to the chemical degradation of melts. In case of polyester, many several degradation mechanisms can happen depending on the processing conditions. Racha Al-Itry *et al.*<sup>13</sup> proposed that the possible mechanisms of thermal degradation of polyester in the processing temperature range between 150 and 210 °C, mainly include hydrolysis and random main-chain scission. The hydrolytic degradation of polyester is primary due to hydrolysis of the ester linkages, which occurs randomly along the backbone of the polyester. The hydrolysis rate hinges on temperature, water

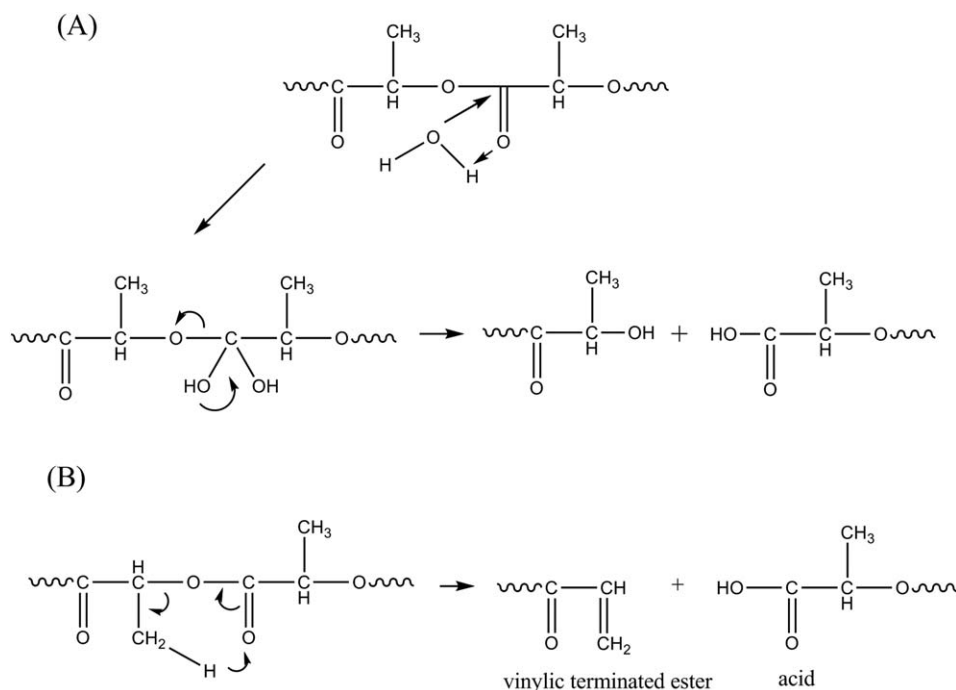


**Figure 3.** Proposed hydrolytic mechanism of PLA (A); and  $\beta$ -C-H Hydrogen transfer of PLA (B).

concentration, and residual catalyst in the resins. The random main-chain scission of polyester at temperature above 180 °C can be attributed to  $\beta$ -C-H hydrogen transfer of polyester, leading to a vinyl ester and acid end groups presented.<sup>13,17</sup> According to the literatures,<sup>13,17</sup> the proposed hydrolytic mechanism and  $\beta$ -C-H Hydrogen transfer of PLA and TPEE are presented in Figures 3 and 4, respectively.

To compensate for such chemical degradation of PLA and TPEE during melting process, the multifunctional epoxide chain extender (ADR) was used. According to the literatures,<sup>13,18</sup> the epoxide groups of ADR can theoretically react with both terminal carboxyl and terminal hydroxyl groups of polyesters. However, in the case of polyester, the reactive activity of hydroxyl groups with epoxide is significantly lower than that of carboxylic acid with epoxide. It means that glycidyl esterification of end -COOH groups precedes end -OH group etherification largely. The proposed chain extension/branching mechanism of PLA/ADR and TPEE/ADR were presented in Figures 5 and 6, respectively.

In order to investigate the chain extension/branching effect of ADR, the torque values were measured as a function of time for PLA/ADR, TPEE/ADR, and PLA/TPEE/ADR (80/20/*x*) with various ADR additions, respectively, as shown in Figure 7. Previous studies have noted a close correlation between the torque values and the increase in molecular size.<sup>19,20</sup> It is pointed that the melt strength and torque value would show an increment with increasing molecular weight. Instead, the decrease in molecular weight resulted from chain scission would lead to a decrease in melt strength and torque value. Hence we consider that this relation can be applied here appropriately.

During the melt mixing process, PLA or TPEE should undergo two opposing reactions, namely, scission reactions due to chemical degradation and chain extension/branching reaction caused

by the presence of ADR. As a result, the chain extension tends to reverse the effect by degradation. Hence, the competing reaction would obviously change the dependency of torque on processing time. As shown in Figure 7(A,B), the torque vs. time plots of PLA/ADR and TPEE/ADR are different with those of blank samples. With increasing ADR addition, the torque values of PLA and TPEE melts increase obviously. Furthermore, when ADR addition is equal or greater than 0.6 phr, three stages (named as I, II, and III) of torque evolution with time are observed in PLA/ADR and TPEE/ADR systems. The first (I) period between 0 and 4.5 min also corresponds to feeding and melting process of resins in the mixing chamber. However, in the second (II) period between 4.5 and 15 min, the torques increase continuously with time, indicating an increase in melt viscosity and molecular size. It can be attributed to the extension/branching reaction prevailing on the scission reactions. And then, the torques increase gradually and finally get approximate balance in the third (III) period. This phenomenon suggests that a dynamic equilibrium between scission reactions and chain extension/branching reactions has been obtained in the third (III) period during mixing process. It is confirmed by the analysis of torque that ADR is an effective modifier for both PLA and TPEE to constrain the chemical degradation, and enhance the melting strength.

In comparison with PLA/ADR and TPEE/ADR samples, PLA/TPEE/ADR (80/20/*x*) blends show a similar dependency of torque on processing time. It indicates that ADR induced an effective chain extension/branching reaction in PLA/TPEE melts. In particular, the chain extension/branching resultants are more complex. Besides the chain extension/branching reactions between PLA/PLA and TPEE/TPEE chains, ADR also can cause coupling reactions between PLA/TPEE chains leading to formation of PLA-ADR-TPEE copolymers, as shown in Figure 8.

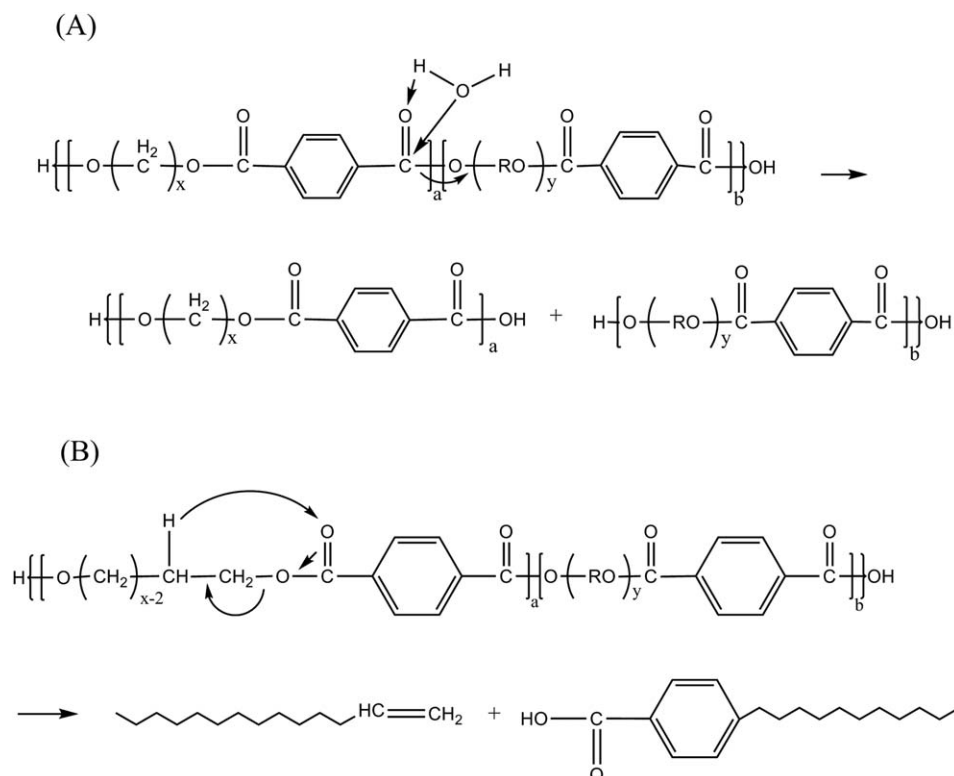


Figure 4. Proposed hydrolytic mechanism of TPEE (A); and  $\beta$ -C-H Hydrogen transfer of TPEE (B).

#### Rheological Properties of PLA/TPEE (80/20) Blend in the Presence of ADR

Furthermore, in order to investigate the chain extension/branching effect of ADR on PLA and TPEE melts, MFRs of PLA/ADR, TPEE/ADR and PLA/TPEE/ADR (80/20/ $x$ ) with various ADR

loadings were measured, respectively, as shown in Figure 9. According to our prior test, the obtained MFR values for neat PLA and TPEE before processing are 3.3 and 6.0 g·10 min<sup>-1</sup>, respectively. As expected, after melt-processing at 190°C for 10 min, the MFR values of neat PLA and TPEE increased to 6.0

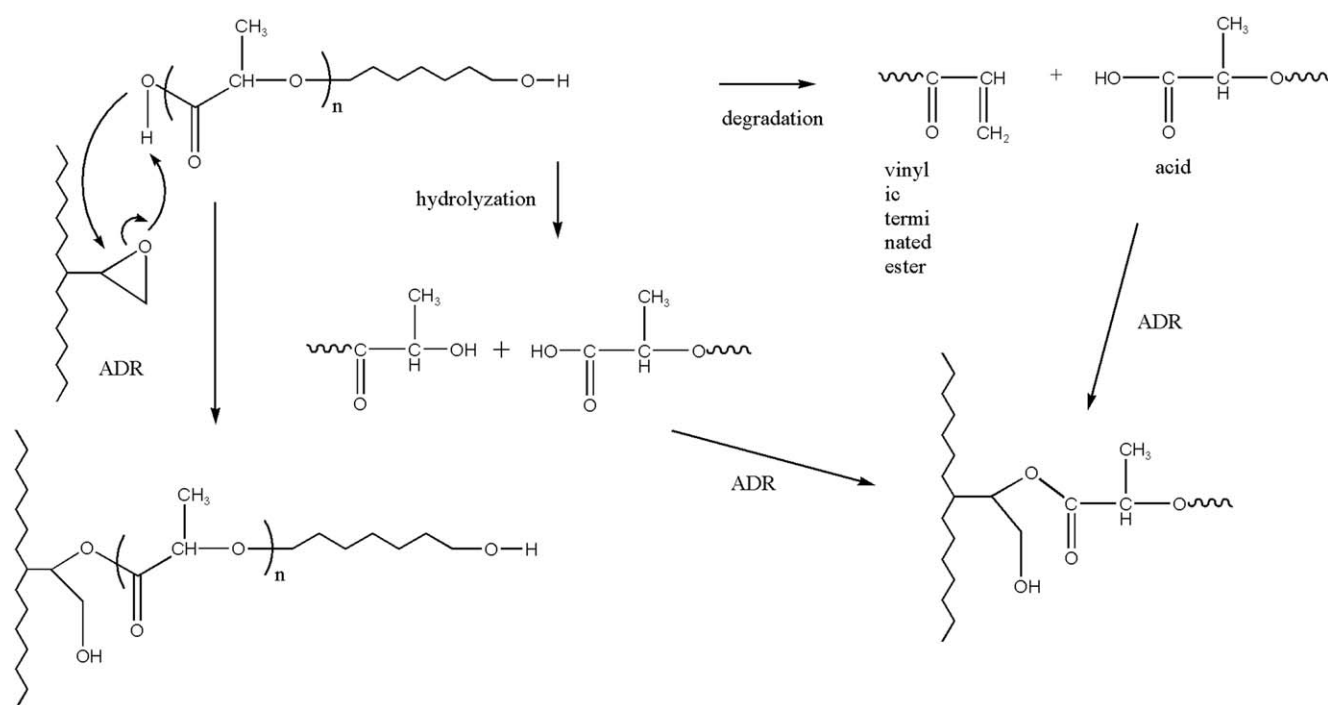
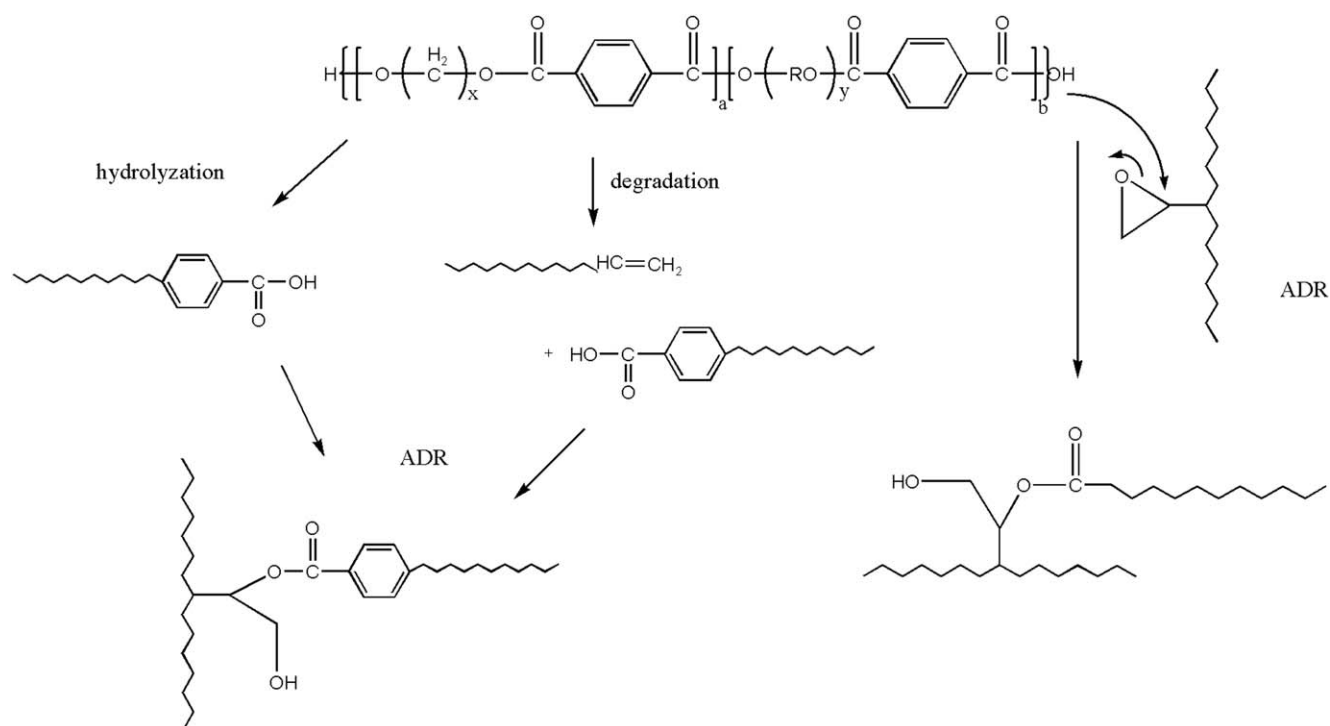


Figure 5. Proposed mechanism of the reaction between PLA and ADR.



**Figure 6.** Proposed mechanism of the reaction between TPEE and ADR.

and  $8.1 \text{ g} \cdot 10 \text{ min}^{-1}$ , respectively. The increase in MFR is attributed to the thermal degradations of polyesters during the melt-processing. However, after PLA melt had been blended with ADR at  $190^\circ\text{C}$  for 10 min, it was found that the MFR value of PLA reduced drastically with the incorporation of ADR. This became more pronounced as the ADR loading increased. When ADR loading increased to 1.2 phr, the MFR of PLA/ADR decreased to  $0.3 \text{ g} \cdot 10 \text{ min}^{-1}$ . For TPEE samples, the similar dependence of MFR on ADR loading also was confirmed from Figure 9. It is well known that MFR value of polymer will decrease when its molecular weight increases. The decrease in MFR, meaning a high viscosity in the PLA and TPEE melts, could be attributed to the occurrence of a chain extension/branching reaction at the presence of ADR, as proposed in Figures 5 and 6. SEC measurement can provide information about molecular weight of macromolecule, which can serve as a parameter to evaluate the macromolecular structure and thermal stability of polyesters at the elevating temperature during the melt-process.  $M_n$ ,  $M_w$  and PDI of PLA and TPEE samples with various ADR loading were listed in Table I. It is found that both  $M_n$  and  $M_w$  for neat PLA decreased after melt-processing at  $190^\circ\text{C}$  for 10min. With increasing the ADR loading, the  $M_n$  and  $M_w$  increased obviously. For example,  $M_n$  and  $M_w$  of neat PLA before processing are  $98 \times 10^3 \text{ g/mol}$  and  $188 \times 10^3 \text{ g/mol}$ , respectively. After ADR of 1.2 phr was blended with PLA melt at  $190^\circ\text{C}$  for 10 min,  $M_n$  and  $M_w$  of the obtained PLA sample increased to  $135 \times 10^3 \text{ g/mol}$  and  $307 \times 10^3 \text{ g/mol}$ , respectively. The increases in  $M_n$  and  $M_w$  are up to 38% and 63%, respectively. Similar to PLA, when melt-blended with ADR at  $190^\circ\text{C}$  for 10 min, TPEE also showed notable increases in  $M_n$  and  $M_w$ , as shown in Table I. The increase in molecular

weight can be attributed to the chemical reaction between epoxide groups of ADR and terminal carboxyl groups of the polyesters, as proposed in Figures 5 and 6. According to the analysis of MFR and SEC measurements, it can be pointed to that ADR is an efficient chain extender for PLA and TPEE. The above results are also consistent with the torque result.

As expected, PLA/TPEE/ADR (80/20/x) blends also show a similar dependency of MFR on ADR loadings. As shown in Figure 9, the MFR decreases obviously with increasing the ADR loading, indicating that the incorporation of ADR increases the viscosity of PLA/TPEE (80/20) blends. With increasing the ADR loading from 0 phr to 0.3 phr, MFR decreases from 8.5 to  $1.7 \text{ g} \cdot 10 \text{ min}^{-1}$ . When ADR loading is 0.9 and 1.2 phr, respectively, MFR of ternary blend is further down to 0.3 and  $0.1 \text{ g} \cdot 10 \text{ min}^{-1}$ . Considering that lack of melt flowability would undermine the processing and forming ability of PLA/TPEE blends, the proper ADR loading should be less than 1.0 phr.

The increase in viscosity of PLA/TPEE/ADR (80/20/x) blends can be attributed to the chain extension/branching reactions. In particular, the chain extension/branching resultants are more complex. Besides the chain extension/branching reactions between PLA/PLA and TPEE/TPEE chains, ADR also can cause coupling reactions between PLA/TPEE chains leading to formation of PLA-ADR-TPEE copolymers, as shown in Figure 8. The copolymer could play a role in compatibilization of PLA/TPEE blends. Hence, ADR not only can be used as a chain extender, but also as a reactive compatibilizer in PLA/TPEE blending system theoretically. Hence, effects of the *in situ* coupling reaction of ADR on compatibility and mechanical performances of PLA/TPEE samples had been researched in the following sections.

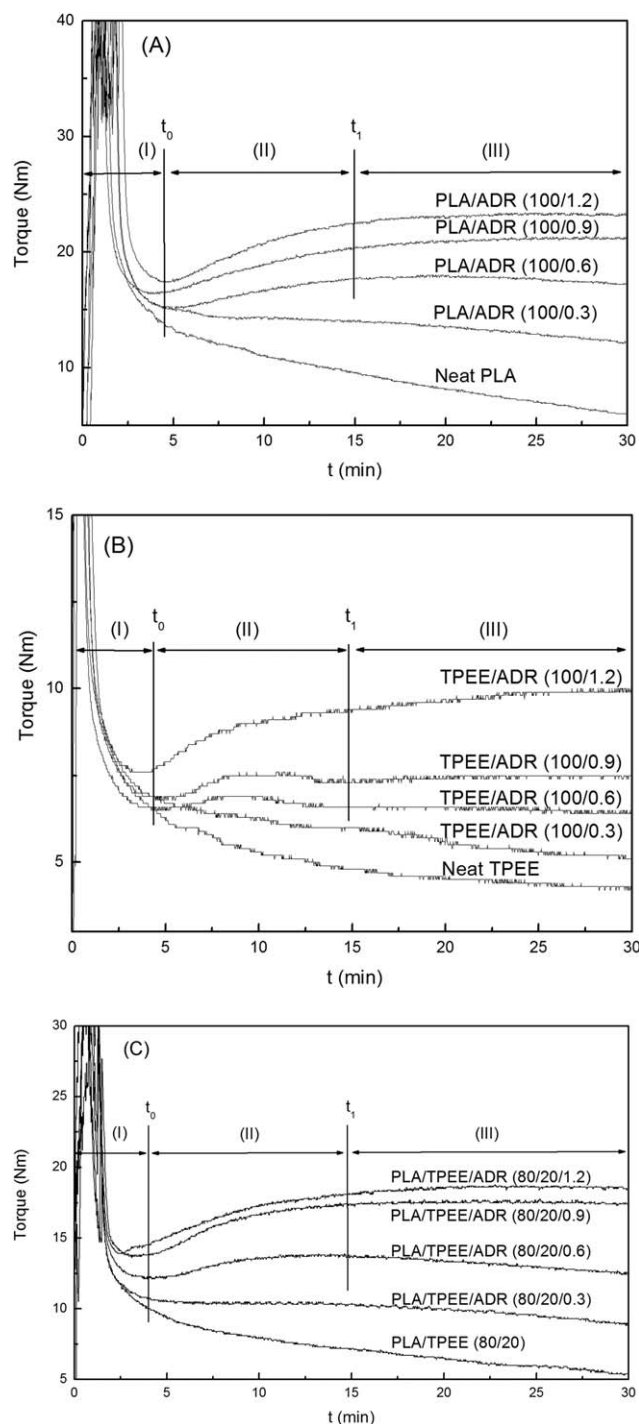


**Figure 7.** Melt torque versus time plots for PLA/ADR (100/ $x$ ) blends (A), TPEE/ADR (100/ $x$ ) blends (B), and PLA/TPEE/ADR (80/20/ $x$ ) blends (C) with different ADR addition.

Of course, due to its multiple epoxy groups, ADR maybe also cause crosslinking reaction while forming partly crosslinking structure accompanied with the chain extension/branching reaction in PLA/TPEE blends. An estimation of the possible crosslinking part content of PLA/TPEE/ADR (80/20/0.6) and PLA/TPEE/ADR (80/20/1.2) samples was performed by dissolving in chloroform solvent at room temperature. After 12 h, it was found that each

sample was fully dissolved. The result presents that a small quantity of ADR could not cause crosslinking reaction between PLA and TPEE during compounding in the molten state. The similar conclusion also was confirmed by the complete dissolubility of PLA/ADR, as well as TPEE/ADR samples in chloroform.

#### Micro-Morphology and Tensile Property of PLA/TPEE/ADR (80/20/ $x$ ) Blends with Various ADR Addition

According to the analysis of torque and MFR, it is confirmed that ADR is an efficient chain extender for PLA/TPEE blend. Considering that ADR would cause the coupling reaction and form some PLA-ADR-TPEE copolymers when PLA, TPEE and ADR were melt-blended, the *in situ* compatibilization effect of ADR on the micro-morphology and physical properties of PLA/TPEE blends has been researched in this article.

To investigate the reactive compatibility of PLA/TPEE/ADR (80/20/ $x$ ) blends with various ADR additions, the cryo-fracture surface of specimens was observed by SEM. The obtained SEM pictures were presented in Figure 10. As shown in Figure 10(A), the PLA/TPEE (80/20) blend without ADR shows a typical “sea island structure”. Moreover, the average TPEE domain size is around 5  $\mu\text{m}$  and an obvious interface debonding phenomenon is observed at the interface between PLA matrix and TPEE particles. It can be attributed to poor compatibility between PLA and TPEE. As shown in Figure 10(B–D), when ADR was incorporated into PLA/TPEE (80/20) blends, it can be found that the TPEE domain size reduced obviously, and the phase interface became blurred significantly. It is due to the fact that ADR can cause coupling reactions between PLA/TPEE chains leading to formation of PLA-ADR-TPEE copolymers which play a role in compatibilization of PLA/TPEE blends. Bao *et al.*<sup>21</sup> blended poly(ethylene terephthalate glycol) (PETG) with PLA using methylene diphenyl diisocyanate (MDI) as a reactive compatibilizer to improve the toughness of PLA. The authors concluded that the active free isocyanate groups on crosslinked PLA could connect the  $-\text{OH}$  of PETG and PLA to form PLA-*co*-PETG copolymer. The PLA-*co*-PETG copolymer could reduce the interfacial tension and increased the interfacial adhesion, thus acting as a compatibilizer.

The tensile strength and elongation at break of neat PLA, TPEE, and PLA/TPEE/ADR (80/20/ $x$ ) samples with various ADR additions were presented in Table II. The dependence of tensile properties on ADR addition and the optical photographs of tensile-fractured samples were given in Figures 11 and 12, respectively. It can be found that the elongation at break of neat PLA is only 2%, showing a classic brittle fracture behavior. By contrast, the elastomer TPEE has a high elongation at break of 886%. However, when 20 wt % TPEE was blended with PLA, the elongation at break of PLA/TPEE (80/20) sample only increased from 2 to 53%. The limited increment in elongation at break of PLA/TPEE (80/20) sample is attributed to the low compatibility of PLA and TPEE resulting in less interfacial adhesion. The less interfacial adhesion would lead to debonding of TPEE particles from PLA matrix and induce premature cracks under tensile stress. Surprisingly, it is found that with even 0.3 phr of ADR the elongation at break of the blend



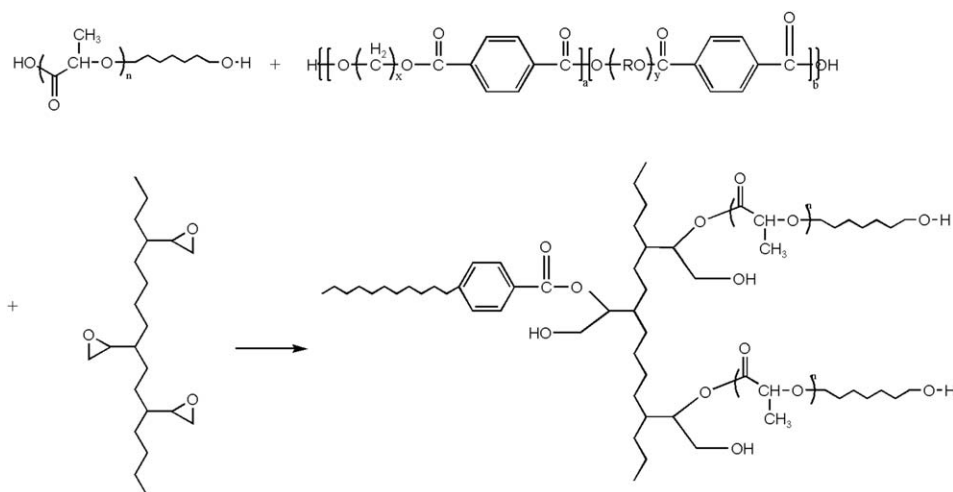


**Figure 8.** Proposed mechanism of the reaction between PLA, TPEE, and ADR.

significantly increased to 193%. And then, the elongation at break slowly increased with further increasing ADR addition.

Similarly, as shown in Figure 12, PLA/TPEE (80/20) sample showed a yielding with subsequent failure immediately with the introduction of tensile load. Compared with PLA/TPEE (80/20) sample, PLA/TPEE/ADR (80/20/*x*) samples showed clear yielding behaviors upon stretching, and then the strain developed continuously. Finally, the samples broke at a significantly increased elongation.

The improvement in tensile ductility of PLA/TPEE/ADR (80/20/*x*) can be explained by the elastomer toughening mechanism. According to Figure 12, it is found that each of PLA/TPEE/ADR (80/20/*x*) samples showed a similar tensile yield behavior. In addition, necking and whitening phenomena were simultaneously found when these samples were cold draw. Hence, the tensile deformation mechanism of PLA/TPEE/ADR (80/20/*x*) blends should be the crazing with shear yielding mechanism. It can be found from Figure 10, the average TPEE domain size is around 5  $\mu\text{m}$  in the blank PLA/TPEE (80/20) sample. With addition of ADR, the TPEE domain size shows an obvious

reduction due to the reactive compatibilization of ADR. According to the crazing with shear yielding mechanism, when the elastomer content is constant, elastomer particles with smaller size will lead to an increase in the number of particles that is helpful to terminate a craze extension and prevent a microscopic crack initiation and propagation, allowing for a considerable plastic deformation to develop.<sup>22</sup> In addition, the enhancement of interfacial adhesion can obviously limit the debonding of TPEE particles from PLA matrix that is also helpful to prevent a premature cracks developing under tensile stress.

From Figure 11, it is also showed that the tensile strength of PLA/TPEE/ADR (80/20/*x*) blends increased slightly with increasing the addition of ADR. The slight increase in tensile strength is attributed to the chain extension of PLA matrix at the present of ADR.

As summarized in Figures 11 and 12, the addition of ADR led to a drastic increase in the elongation at break. The PLA/TPEE (80/20) blend achieved high tensile ductility without tensile strength loss by the *in situ* compatibilization reaction with ADR.

### DSC Analysis

The crystallization and melting behaviors of PLA/TPEE/ADR (80/20/*x*) blends with various ADR additions were investigated

**Table I.** SEC Data of PLA and TPEE Blended with Various ADR Loading at 190 °C for 10 min

Sample	$M_n/10^3$ (g/mol)	$M_w/10^3$ (g/mol)	PDI
PLA pellet	98	188	1.9
PLA processed	89	153	1.7
PLA/ADR (100/0.6)	116	254	2.2
PLA/ADR (100/1.2)	135	307	2.3
TPEE pellet	38	61	1.6
TPEE processed	32	61	1.9
TPEE/ADR (100/0.6)	67	146	2.2
TPEE/ADR (100/1.2)	89	191	2.1

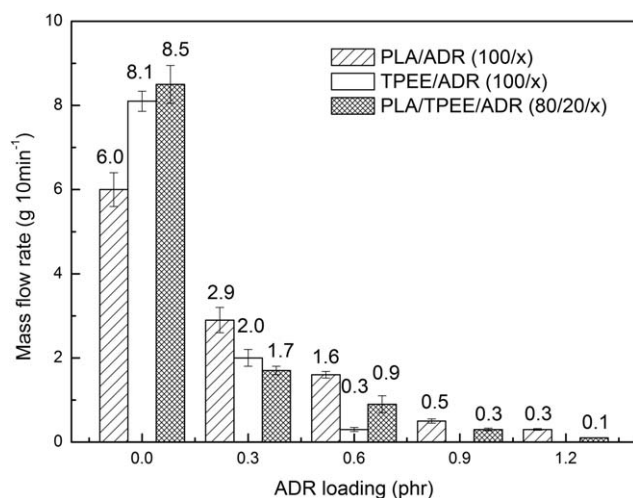


**Figure 9.** Effect of ADR addition on MFR of PLA/ADR(100/*x*), TPEE/ADR(100/*x*), and PLA/TPEE/ADR (80/20/*x*) samples.

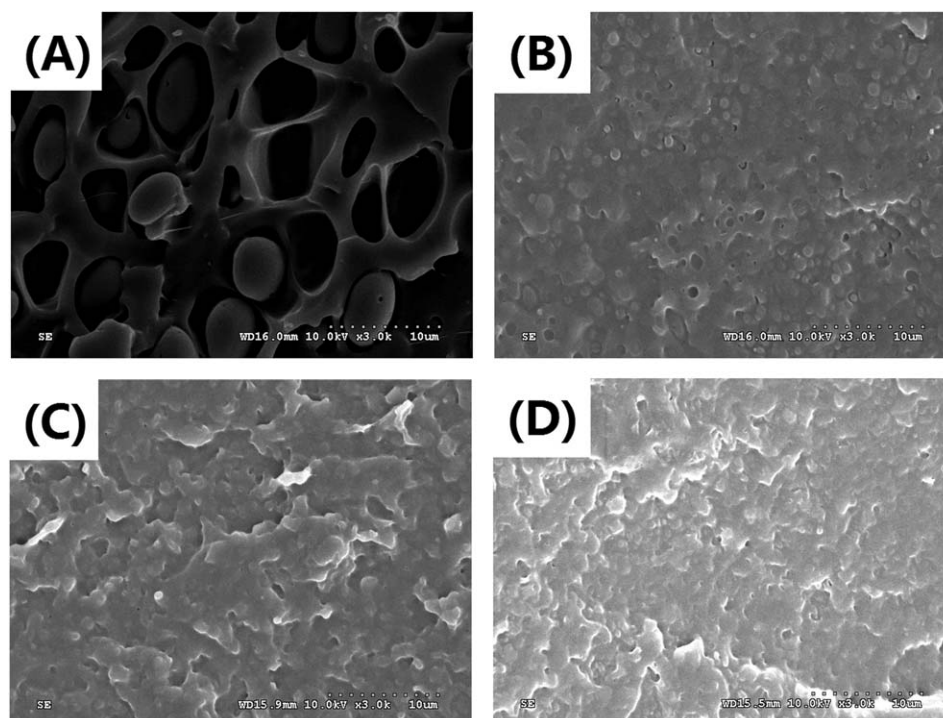


**Figure 10.** SEM pictures of cryo-fracture of PLA/TPEE/ADR blends (A) PLA/TPEE (80/20); (B) PLA/TPEE/ADR (80/20/0.3); (C) PLA/TPEE/ADR (80/20/0.6); (D) PLA/TPEE/ADR (80/20/1.2).

by DSC. DSC thermograms for PLA/TPEE/ADR (80/20/*x*) samples cooled at 10 °C/min and subsequently heated at 10 °C/min are shown in Figure 13(A,B), respectively. The obtained thermal parameters are also listed in Table III.

As indicated in Figure 13(A), PLA does not exhibit a crystallization peak upon cooling due to its weak melt-crystallization ability.<sup>23</sup> Similar to neat PLA, there is no obvious crystallization peak observed yet for PLA/TPEE (80/20) and PLA/TPEE/ADR (80/20/*x*) samples, indicating that the addition of TPEE and ADR has no obvious effect to increase the melt-crystallization rate of PLA matrix when PLA melt was cooled down at a cooling rate of 10 °C/min.

However, as shown in Figure 13(B), each sample shows a strong exothermic peak in the respective DSC thermogram obtained for subsequently heated at 10 °C/min. The exothermic peak is attributed to cold crystallization of PLA matrix in amorphous

solid state during the subsequent heating DSC scanning. Neat PLA and PLA/TPEE (80/20) sample represent the cold crystallization peak ( $T_{cc}$ ) at 103.3 °C and 105.8 °C, respectively. Interestingly, with increasing the ADR addition,  $T_{cc}$  of PLA/TPEE/ADR (80/20/*x*) samples increases slightly indicating that the cold-crystallization ability of PLA matrix is weakened. It can be attributed to the fact that the insertion of ADR segments and the formation of irregular branched structure in PLA chains would constrain the conformational mobility of PLA chains required for the spherulitic growth. In addition, according to the SEC result, the marked increase in molecular weight of PLA due to the chain extension reaction also weakened the cold-crystallization ability of PLA.

**Table II.** Tensile Properties of PLA/TPEE/ADR (80/20/*x*) Blends

Samples	Tensile yield strength (MPa)	Elongation at break (%)
PLA	56.2	2
TPEE	29.0	886
PLA/TPEE (80/20)	42.8	53
PLA/TPEE/ADR (80/20/0.3)	44.0	193
PLA/TPEE/ADR (80/20/0.6)	44.8	195
PLA/TPEE/ADR (80/20/0.9)	44.3	199
PLA/TPEE/ADR (80/20/1.2)	46.0	213

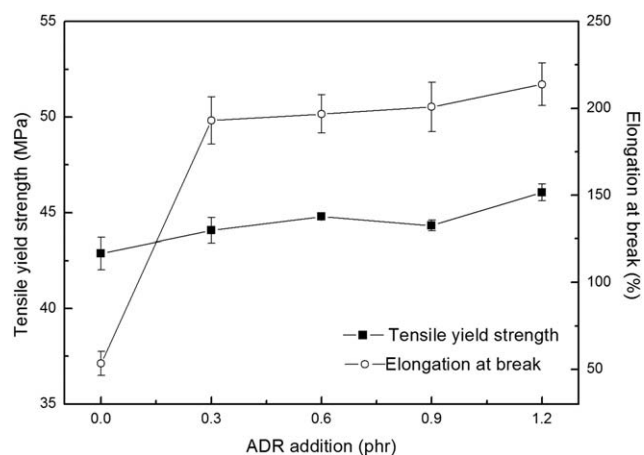


**Figure 11.** Elongation at break and tensile strength of PLA/TPEE/ADR.

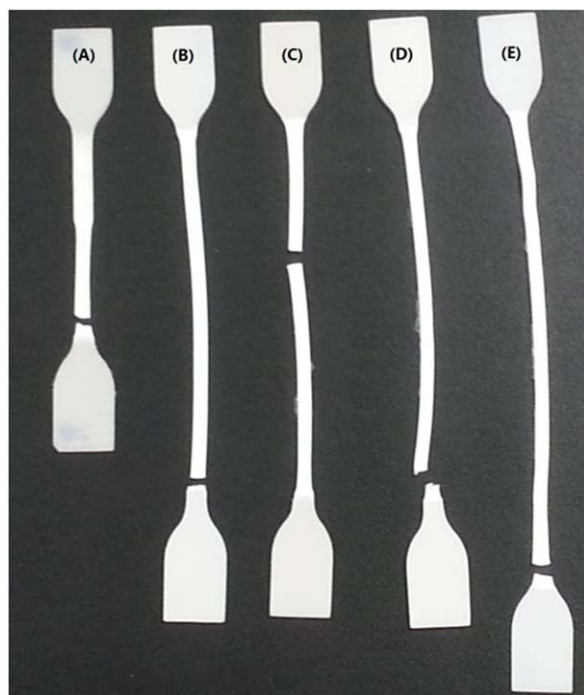


**Figure 12.** Optical photographs of tensile-fractured samples. (A) PLA/TPEE (80/20); (B) PLA/TPEE/ADR (80/20/0.3); (C) PLA/TPEE/ADR (80/20/0.6); (D) PLA/TPEE/ADR (80/20/0.9); (E) PLA/TPEE/ADR (80/20/1.2). [Color figure can be viewed in the online issue, which is available at [wileyonlinelibrary.com](http://wileyonlinelibrary.com).]

Moreover, it can be concluded from Table III that the incorporation of TPEE with and without ADR has almost no influence on glass transition temperature ( $T_g$ ) and melting temperature ( $T_m$ ).

Notably, cold crystallization enthalpy ( $\Delta H_{cc}$ ) of PLA matrix indicates an obvious reduction with increasing the ADR addition. When ADR addition increases from 0 phr to 0.9 phr,  $\Delta H_{cc}$  of PLA matrix in PLA/TPEE blend decreases from 29.6 J/g to 23.3 J/g. The decrease in  $\Delta H_{cc}$  also suggests that the irregular and branching PLA chains might decrease the cold crystallization ability required for crystal growth. It is consistent with the result of  $T_{cc}$ . In addition, for each sample, the melting enthalpy ( $\Delta H_m$ ) is slightly larger than the corresponding  $\Delta H_{cc}$ . It suggests that the melted crystalline structures corresponding to  $\Delta H_m$  almost formed during the cold crystallization process [as shown in Figure 13(B)], and the crystal quantity formed during the melt-crystallization process is very few [as shown in Figure 13(A)]. As a result, the crystallinity of PLA matrix in neat PLA and PLA/TPEE/ADR (80/20/ $x$ ) samples is only around 3.0%, indicating that PLA matrix would be amorphous when these PLA blend melts are cooled to room temperature at a cooling rate of 10 °C/min.

From Figure 13(B), it has to be pointed to that neat TPEE shows a weak and broad melting endothermic peak at around 175 °C with a very low melting enthalpy of 1.5 J/g. For PLA/TPEE (80/20) sample, the weak endothermic peak of TPEE component was superposed completely by the strong endothermic peak of PLA matrix at around 169 °C. Hence, the measured

value of  $\Delta H_m$  for PLA matrix is slightly higher than the true value of  $\Delta H_m$ . As a result,  $X_c$  of 3.7% for the PLA/TPEE (80/20) blend is slightly higher than that (3.3%) for neat PLA, as presented in Table III. In other words, the measured value of  $X_c$  for PLA matrix in PLA/TPEE (80/20) sample is slightly higher than the true value of  $X_c$ .

#### Blown Film of PLA/TPEE/ADR(80/20/ $x$ ) Blends

Attempts were made to produce ductile films from these PLA/TPEE/ADR (80/20/ $x$ ) blends by using extrusion blowing method. Effect of ADR on blowing stability and tensile property of PLA/TPEE blends was investigated. Figure 14 presents the comparison of the bubble shape between PLA, PLA/TPEE (80/20), PLA/TPEE/ADR (80/20/0.3) and PLA/TPEE/ADR (80/20/0.6) samples. It is found from Figure 14(A,B) that PLA and PLA/TPEE (80/20) blend without ADR shows an unstable behavior during their blown extrusion processing. As shown in Figure 14(C,D), when 0.3 and 0.6 phr ADR were incorporated into PLA/TPEE (80/20) blends, respectively, a significant improvement in the blowing stability was achieved. Due to weaker melt strength resulted from thermal degradation of PLA

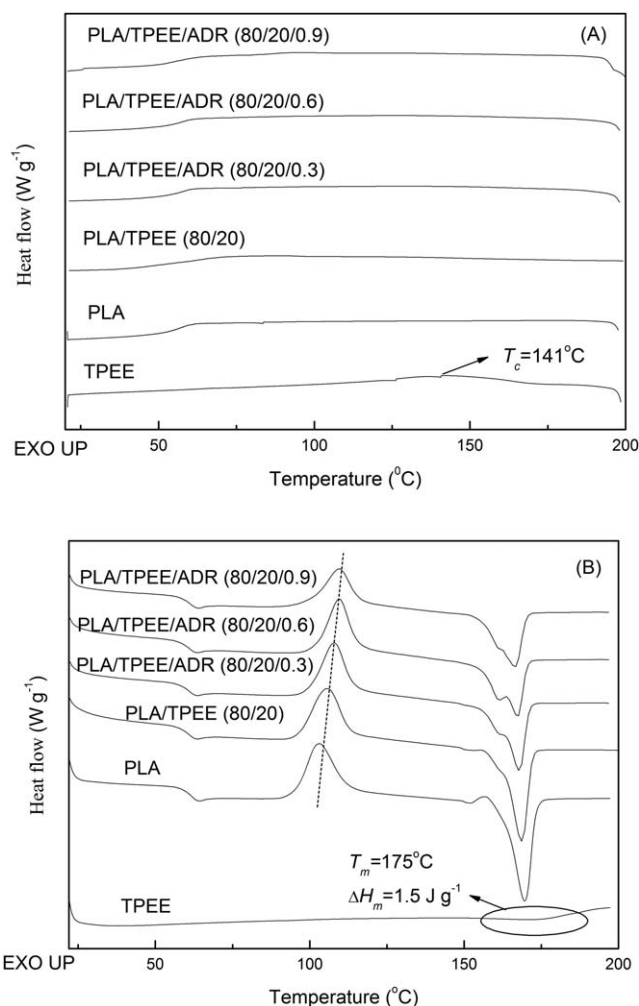


**Figure 13.** The first cooling DSC traces (A) and the sequential heating DSC traces (B) of PLA samples.

**Table III.** DSC Data of Neat PLA and PLA Blends from Thermalgrams

Sample	$T_g$ (°C)	$T_{cc}$ (°C)	$T_m$ (°C)	$\Delta H_{cc}$ (J·g <sup>-1</sup> )	$\Delta H_m$ (J·g <sup>-1</sup> )	$X_c$ (%)
PLA	62.0	103.3	167.9	30.1	33.2	3.3
PLA/TPEE (80/20)	61.5	105.8	168.6	29.6	33.0	3.7
PLA/TPEE/ADR (80/20/0.3)	61.4	107.9	167.7	27.3	30.4	3.3
PLA/TPEE/ADR (80/20/0.6)	61.1	109.5	167.4	25.5	28.5	3.2
PLA/TPEE/ADR (80/20/0.9)	61.6	109.6	166.5	23.3	26.0	2.9

and TPEE melts, the formation of a stable bubble during extrusion blowing was more difficult. However, with the incorporation of ADR, the melt strength of PLA/TPEE blend was

enhanced due to the chain extension/branching reaction of ADR with PLA and TPEE chains. Consequently, the stability on extrusion blowing of PLA/TEPP (80/20) blend was enhanced

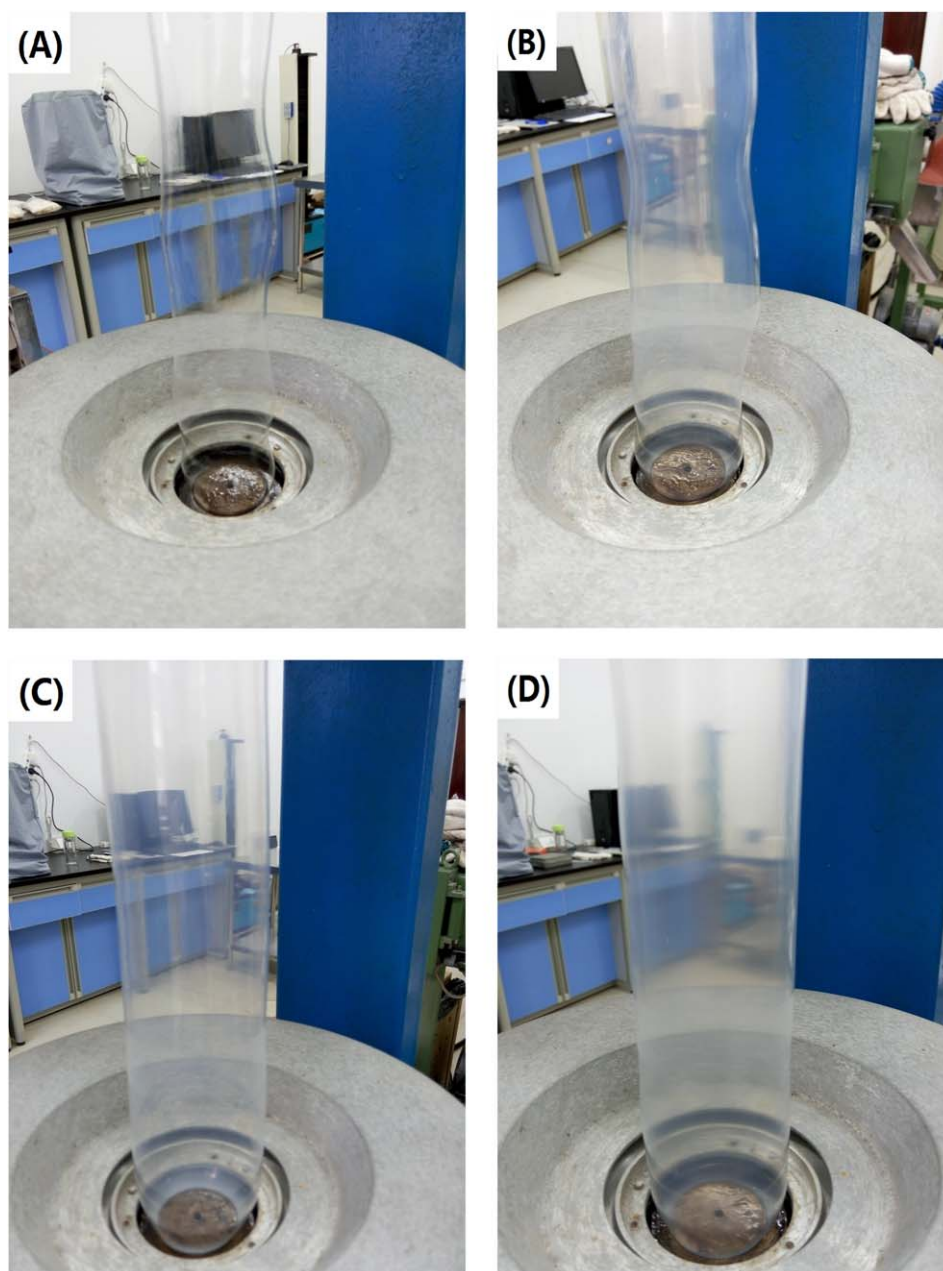


**Figure 14.** Comparison of the bubble shape between (A) neat PLA, (B) PLA/TPEE (80/20), (C) PLA/TPEE/ADR (80/20/0.3), and (D) PLA/TPEE/ADR (80/20/0.6). [Color figure can be viewed in the online issue, which is available at [wileyonlinelibrary.com](http://wileyonlinelibrary.com).]

**Table IV.** Tensile Properties of the Blown Films of PLA/TPEE (80/20), PLA/TPEE/ADR (80/20/0.3) and PLA/TPEE/ADR (80/20/0.6) Blends

Film sample	Tensile strength (MPa)		Elongation at break (%)	
	MD	TD	MD	TD
PLA/TPEE (80/20)	40.5	18.3	185.6	14.6
PLA/TPEE/ADR (80/20/0.3)	39.9	28.8	397.8	111.8
PLA/TPEE/ADR (80/20/0.6)	41.1	26.5	374.0	124.6

obviously. As reported in literature,<sup>24,25</sup> Organic peroxy compound and a copolymer of styrene, methyl methacrylate and glycidyl methacrylate were used as viscosity enhancers to enhance PLA melt strength. These additives protect PLA melt from degradation and couple polymer chains to attenuate overall loss of molecular weight and viscosity of PLA melt. As a result, a stable bubble of PLA during extrusion blowing was achieved.

In addition, the tensile performance of blown films of PLA/TPEE (80/20), PLA/TPEE/ADR (80/20/0.3) and PLA/TPEE/ADR (80/20/0.6) blends were presented in Table IV. As expected, the tensile performance of PLA/TPEE (80/20) films was improved with the incorporation of ADR. Notably, both the elongation at breaks in MD and TD show a significant increase when ADR was incorporated into PLA/TPEE (80/20) film, compared with those of PLA/TPEE (80/20) film without ADR. The improvement in tensile ductility of PLA/TPEE/ADR films is attributed to the fact that the *in situ* coupling reaction of PLA and TPEE at the presence of ADR can enhance the compatibility of PLA matrix and TPEE domain. It must be pointed out that the tensile strength and elongation at break in TD are obviously less than those in MD for each film sample, which maybe resulted from a minor blow-up ratio (around 2:1).

In our follow-up research, the effects of ADR loading, as well as processing parameters, on the stability of blown extrusion process, micro-morphology, thermal and mechanical properties will be researched systematically.

## CONCLUSIONS

In this article, PLA-based tough materials are prepared by reactive blending with TPEE in the presence of a multifunctional epoxide oligomer (ADR). *In situ* reactions between PLA, TPEE and ADR were researched using a lab torque rheometer. Torque rheometer and MFR measurements indicate that the incorporation of ADR markedly increased the melt viscosity of PLA/TPEE (80/20) blends. It is proposed that ADR may initiate a variety of chain extension/branching reactions between PLA and TPEE under mixing process. In particular, the formed copolymer PLA-ADR-TPEE could be viewed as an *in situ* compatibilizer to improve the compatibility of PLA and TPEE. The morphology reveals that the *in situ* compatibilization led to a reduction in TPEE domain size and an enhancement in their interfacial adhesion. Moreover, tensile ductility of PLA/TPEE (80/20) blend was improved greatly by the incorporation of

ADR. It is found that with even 0.3 phr of ADR the elongation at break of the PLA/TPEE (80/20) blend significantly increased from 53 to 193%. And then, the elongation at break slowly increased with further increasing the ADR addition. The crazing with shear yielding mechanism is considered to be the dominating toughening mechanism for these PLA/TPEE/ADR blends. In addition, the DSC result display that the thermal properties of PLA/TPEE (80/20) blend were not affected obviously by the incorporation of ADR. Considering that lack of melt flowability would undermine the processing and forming ability of PLA/TPEE blends, the proper ADR addition should be less than 1.0 phr.

Attempts were made to produce ductile films from these PLA/TPEE/ADR blends by using extrusion blowing method. Effect of ADR on blowing stability and tensile property of these blends was investigated. Improvement on blowing stability and tensile ductility of PLA/TPEE/ADR films can be attributed to the fact that the *in situ* coupling reaction of PLA and TPEE at the presence of ADR enhances the melt strength and the compatibility of PLA and TPEE.

## ACKNOWLEDGMENTS

The authors gratefully acknowledge support from Hainan University of 211 Project, Hainan University graduate-student joint training project in the discipline of materials science and engineering, and Analytical and Testing Center of Hainan University. The authors also thank the support from National Science Foundation of China (grant number: 51263007), Natural Science Foundation of Hainan Province of China (grant number: 514206), and Youth science fund of Hainan University (grant number: qnjj1232).

## REFERENCES

- Rasal, R. M.; Janorkar, A. V.; Hirt, D. E. *Prog. Polym. Sci.* **2010**, *35*, 338.
- Liu, H. Z.; Zhang, J. W. *J Polym. Sci. Part B: Polym. Phys.* **2011**, *49*, 1051.
- Lim, L.; Auras, T.; Rubino, R. M. *Prog. Polym. Sci.* **2008**, *33*, 820.
- Li, Y. J.; Shimizu, H. *Macromol. Biosci.* **2007**, *7*, 921.
- Han, L. J.; Han, C. Y.; Dong, L. S. *Polym. Compos.* **2013**, *34*, 122.
- Han, L. J.; Han, C. Y.; Zhang, H. L.; Chen, S.; Dong, L. S. *Polym. Compos.* **2012**, *33*, 850.
- Chen, Y. Y.; Geever, L. M.; Higginbotham, C. L.; Devine, D. M. *Appl. Mech. Mater.* **2014**, *679*, 50.
- Harada, M.; Ohya, T.; Iida, K.; Hayashi, H.; Hirano, K.; Fukuda, H. *J Appl. Polym. Sci.* **2007**, *106*, 1813.
- Jiang, L.; Wolcott, M. P.; Zhang, J. W. *Biomacromolecules* **2006**, *77*, 199.
- Zaman, H. U.; Song, J. C.; Park, L.-S.; Kang, I.-K.; Park, S.-Y.; Kwak, G.; Park, B.; Yoon, K.-B. *Polym. Bull.* **2011**, *67*, 187.
- Cevdet, K.; Yelda, M. *Polym. Adv. Technol.* **2014**, *25*, 1622.
- Zhang, N.; Wang, Q.; Ren, J.; Wang, L. *J. Mater. Sci.* **2009**, *44*, 250.

13. Al-Itry, R.; Lamnawar, K.; Maazouz, A. *Polym. Degrad. Stab.* **2012**, *97*, 1898.
14. Arruda, L. C.; Magaton, M.; Bretas, R. E. S.; Ueki, M. M. *Polym. Test.* **2015**, *43*, 27.
15. Zhang, W. Y.; Gui, Z. Y.; Lu, C.; Cheng, S. J.; Cai, D. X.; Gao, Y. *Mater. Lett.* **2013**, *92*, 68.
16. Fischer, E. W.; Sterzel, H. J.; Wegner, G. *Colloid. Polym. Sci.* **1973**, *251*, 980.
17. Södergård, A.; Näsman, J. H. *Polym. Degrad. Stab.* **1994**, *46*, 25.
18. Japon, S.; Luciani, A.; Nguyen, Q. T.; Letierrier, Y.; Månson, J.-A. E. *Polym. Eng. Sci.* **2001**, *41*, 1299.
19. Silva, S. M. L.; Dias, M. L.; Azuma, C. J. *Polym. Eng.* **2001**, *21*, 543.
20. Jacques, B.; Devaux, J.; Legras, R.; Nield, E. *Polymer* **1997**, *38*, 5367.
21. Bao, R. Y.; Jiang, W. R.; Liu, Z. Y.; Yang, W.; Xie, B. H.; Yang, M. B. *RSC Adv.* **2015**, *55*, 34821.
22. Bucknall, C. B.; Clayton, D.; Keast, W. E. *J. Mater. Sci.* **1972**, *77*, 1443.
23. Wei, T. Y.; Pang, S. J.; Xu, N.; Pan, L. S.; Zhang, Z. Q.; Xu, R. Z.; Ma, N. S.; Lin, Q. *J. Appl. Polym. Sci.* **2014**, *131*, 41308.
24. Sodergard, A.; Selin, J-F; Niemi, M.; Johansson, C-J; Meinander, K. Processable Poly(hydroxyl acid). U.S. Pat. 6,559, 244B1 (**2003**).
25. Tweed, E. C.; Stephens, H. M.; Riegert, T. E. Polylactic Acid Blown Film and Method of Manufacturing Same. U.S. Pat. 7,615,183B2 (**2009**).